

The Sunspot Cycle and Solar Magnetic Fields. II* The Interaction of Flux Tubes with the Convection Zone

Ronald G. Giovanelli

Division of Applied Physics, CSIRO,
P.O. Box 218, Lindfield, N.S.W. 2070.

Abstract

Mechanisms of interaction between flux tubes or ropes and the convection zone are examined insofar as they are relevant to the sunspot cycle. These include floating, transport, and the penetration of gas from outside the tubes. It is found that all previous studies contain one or more major errors of physics which render their conclusions invalid. The errors include invariably the assumption that Archimedes' principle is applicable to flux ropes, that gas entry can be disregarded, and usually that floating criteria depend solely or primarily on local phenomena. Some of the results presented here are explanations of (i) the transport of flux tubes by the slow observed poleward motions and the even slower systems which carry extensions of these tubes downwards to depths of ~ 150 Mm and then equatorwards; (ii) their magnetic field strengths ($\sim 10^4$ G at a depth 10 Mm to $(6-12)\times 10^4$ G at ~ 150 Mm); and (iii) the amplitudes of the torsional oscillation. Taken in conjunction with Part I, where the mechanism of polar field reversal is described and the variation of the phase of the torsional oscillation explained, all major cycle observations are accounted for in what turns out to be a new type of dynamo mechanism.

1. Introduction

The following account deals with physical processes involved in interactions between magnetic flux tubes and their surroundings in the solar convection zone, such as are related to the sunspot cycle. A general mechanism for the cycle itself has been outlined in a companion paper (Giovanelli 1985; hereafter called Part I, see present issue p. 1045). Here we first study processes whereby flux tubes deep in the convection zone develop instabilities and become twisted together to form flux ropes. Conditions are then examined for the floating of sections of these to form sunspots. Mechanisms for the transport to polar regions by the observed weak polewards flow of 20 m s^{-1} of flux tubes are then discussed, together with their further transport deep into the convection zone in polar regions, and from there equator-wards. The processes controlling the field strengths in the flux tubes are also studied, and finally the interaction between the tubes and their surroundings which is responsible for the torsional oscillation.

Some aspects of these problems have been discussed many times over the past quarter of a century. All accounts include at least one fundamental error of physics,

* Part I, *Aust. J. Phys.*, 1985, 38, 1045.

namely the use of Archimedes' principle to test for the ability of a flux tube to float. This principle is not applicable to flux tubes, for which the test of the change in potential energy must be made. The results are greatly different and, as a consequence, all previous work in this area becomes invalid. Again, most accounts consider only a portion of a tube, as if it could be isolated from the whole tube; Spruit's (1981) analyses are however outstanding exceptions. Inadequate attention has been paid to the fundamental role of convective motions in controlling the behaviour of individual flux tubes, and none at all to the effects of gas entry into the tubes, decisive for establishing the equilibrium field strengths.

As in Part I, the present analysis is based largely on observation. Although discussed using only simplified models, the interactions yield results in quantitative agreement with surface observations, with all major observations of the sunspot and magnetic cycles receiving explanations here or in Part I.

2. Physical Conditions in Flux Tubes and the Convection Zone

For the convection zone we adopt Spruit's (1974) model, the depth of which is 198.4 Mm, while the tabulated values are at equal pressure ratios. For convenience we refer to the levels 200, 155, 100, 62 and 10 Mm, which are all close to tabulated values; the calculations use Spruit's actual values.

The magnetic flux and therefore Ba^2 is invariant along a tube of force, B being the longitudinal component of the field and a the tube radius. Whenever flux tubes are twisted only very gently so that the field lines make angles ≤ 0.01 rad with the axis, the magnetic pressure is effectively $B^2/8\pi$ [Piddington (1976*b*) has pointed out that this is the sort of condition appropriate to subsurface flux tubes]. The requirement of pressure balance then leads to

$$B^2 = 8\pi(1-q)p_e, \quad (1)$$

where p_e is the external gas pressure and q the ratio of the internal gas pressure p_i to p_e . From the constancy of flux, we have

$$a_2^2 = a_1^2 B_1/B_2 = a_1^2 \left(\frac{1-q_1}{1-q_2} \frac{p_1}{p_2} \right)^{\frac{1}{2}}, \quad (2)$$

where the subscripts refer to different levels on the one occasion, or after any changes whatsoever regarding tube shape or mass redistribution within the tube. The ratio q is usually very close to unity; for example, at a depth 155 Mm, $1-q = 1.5 \times 10^{-7}$ if $B = 10^4$ G, or 3.5×10^{-5} if $B = 1.5 \times 10^5$ G, more than straddling the range of B to be expected in our later discussion. At 10 Mm, we have $1-q \approx 6 \times 10^{-4}$ for $B \approx 10^4$ G.

Can surface observations provide useful leads as to the values of q ? The only observational determination of q for sunspot umbras and outside is that of Giovanelli (1982), with a value of 0.25 at a depth of about 610 km below $\tau_c = 1$ in the photosphere. At this level, the pressure scale height H_p is 360 km in the external medium. In the umbra where T is much lower, H_p is closer to 115 km. We do not know how rapidly T increases downwards under the umbra. As typical umbral diameters usually exceed 5000 km, it is difficult to see how the characteristic depth to

which this ratio of scale heights of 3.1 applies could be as small as 1000 km. Yet in such a distance, the external pressure p_e increases by over seven times, whereas with a constant ratio of scale heights the pressure under the umbra would increase by over 450 times. Clearly the temperature structure is highly localized, with q increasing rapidly to a value near unity.

There is no observational value of q for the magnetic elements away from sunspots, though it must be much less than unity at some appropriate level in the cavity where the field is concentrated. We can only suppose that, in the isolated tubes which originate from the fragmentation of sunspots, q again increases rapidly with depth and approaches unity quite near the surface.

In non-magnetic regions in the convection zone, the pressure and density ρ at height h above some reference level z_0 , where $h = 0$ and the pressure and density are P_0 and ρ_0 , are given by

$$P = P_0 \exp\left(-\int_0^h dj/H_p\right), \quad \rho = \rho_0 \exp\left(-\int_0^h dj/H_\rho\right). \quad (3, 4)$$

Here H_ρ is the density scale height, j is an alternative symbol for height above z_0 , while z and j are positive outwards. Where there is no confusion, we often drop the subscript from symbols relating to the external medium.

The gas pressure in a magnetic tube is qp . Hydrostatic equilibrium requires that

$$p_i = q_0 p_0 \exp\left(-\int_0^h dj/H_{pi}\right), \quad (5)$$

where the subscript i refers to values within the tube. Although q is close to unity, it may vary with height depending on internal temperature. We now examine two special cases between which, as shown later, the real conditions usually lie.

Case 1. If the tube and its surroundings are at equal temperatures at every level, then we have

$$T_i = T_e. \quad (6)$$

To some accuracy, T/μ is also the same inside and outside the tube, μ being the mean atomic weight, so that

$$H_p = kT/\mu Mg = H_{pi},$$

where M is the mass of unit atomic weight. Then q is independent of height. Further we have $p = \rho kT/\mu M$, so that $\rho_i/\rho = p_i/p$, and

$$\rho_i = qp. \quad (7)$$

Case 2. Piddington (1976*b*) has pointed out that only minor differences are required between T_i and T_e to ensure uniform B over a limited but possibly quite large range of heights. Such differences could be associated only with adiabatic changes in internal gas pressure. In Section 5*d*, the thermal relaxation time is shown to be quite long, so that the adiabatic changes are quasi-stable.

For B uniform with height, Piddington gave the equivalent of

$$T_i/T_e = p_i/p_e = 1 - B^2/8\pi p_e, \quad (8)$$

$$\rho_i = \rho_e. \quad (9)$$

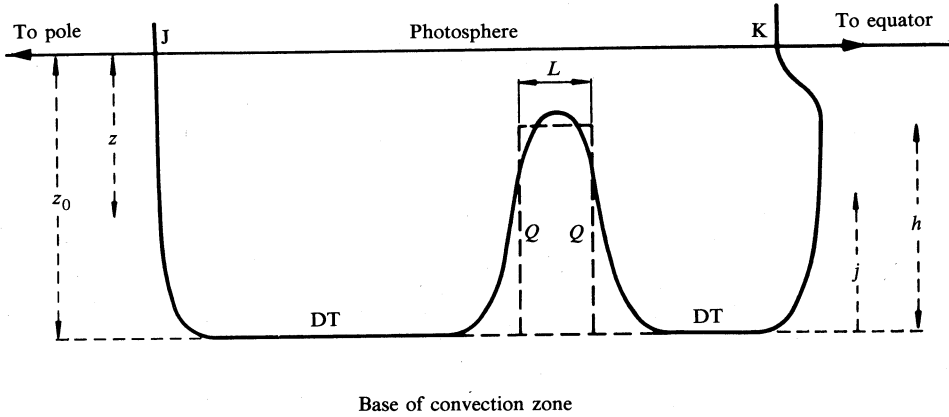


Fig. 1. Simplified flux tube projected onto a meridional plane, extending from a magnetic element in polar regions at J, down into the lower convection zone where it is carried equatorwards at K by the return flow. A perturbation projects upwards to form a loop.

3. Forces on Flux Tubes

Fig. 1 shows schematically a flux tube passing through the surface at two different latitudes and going deep into the convection zone (in practice, the deep tube spirals around the Sun). A section is perturbed upwards to form a loop. Here we consider the conditions under which the tube will float upwards.

Any change in the geometry of the tube involves an internal redistribution of pressure and mass. The floating is fairly rapid, during which any inward diffusion of plasma from outside can be safely disregarded, and thus the mass in the entire tube is conserved.

The consequent redistribution of pressure is not instantaneous, but adjustments occur at a rate approaching the speed of sound $\sim 100 \text{ km s}^{-1}$ throughout much of the convection zone. Delay times of the order of an hour or so may be involved. If the process is continuous, it is virtually as if the reaction were instantaneous, and this is what we assume here.

There are also transients of various origins. To a large extent, oscillatory pressure fluctuations in the magnetic tube will give rise to waves propagating outwards into the non-magnetic exterior, thus damping out the oscillations in the tube. Further, when any portion of a flux tube rises or falls, the ambient pressure changes and the tube diameter increases or decreases. Accompanying this there is, for example, a mass decrease in a rising portion of a tube because the density decreases more rapidly than the pressure. In this case the gas expands downwards. Because the thermal relaxation time is quite long, the temperature regime thus established is effectively

static. Therefore, the only change in the mass distribution within the tube is due to the pressure redistribution. These changes are associated with changes in q and result in important changes in the potential energy PE. It is the change in PE which decides whether or not floating may occur.

The simplest way to assess PE is to refer to a zero where no flux tube is present. If a tube of volume γ is now introduced into the Sun at a given level, a volume of gas $\gamma(1 - q)$ is effectively expelled from γ into the surrounding medium, with PE being increased by $p\gamma(1 - q)$. This expression takes full account of all energy changes, including the effects of magnetic tension. Since PE depends on q explicitly, it is essential first to calculate changes in q as a function of changes in tube geometry before changes in PE can be calculated. As the behaviour depends on the temperature distribution within the flux tube, cases 1 and 2 are considered separately.

There is also a force due to the resistance to motion through the surrounding gases. The standard experimental result for aerodynamic drag, $C\rho v^2 aL$, was introduced into astrophysics by Parker (1955). Here v is the component of gas motion normal to the flux tube axis and $C \approx 1$. Parker (1979) has discussed the variation of C with v , although his analysis has application mainly to superficial layers. In a static medium, aerodynamic drag does not influence whether a flux tube rises or sinks, although it decides the rate at which this occurs.

4. Floating of Flux Tubes: Case 1 where $T_i = T_e$

(a) Stability of Unperturbed Circular Tube of Force and Location of Flux Tubes in the Deep Equatorward Flow

We consider first the stability of an unperturbed flux tube in the lower convection zone, and specifically whether it tends to float or sink. In general, such a tube is wound spirally around the Sun. As a model, we take a purely circular tube concentric with the Sun. If the tube rises uniformly, the radius of its axis R increases by ΔR , and the change in PE is

$$\Delta PE = p_* \gamma_*(1 - q_*) - p_0 \gamma_0(1 - q_0), \tag{10}$$

where the subscript zero refers to the initial value and the asterisk to the new value.

To obtain q_* , it is necessary to use the principle of mass invariance described in Section 3. The procedure, which recurs usually with increasing complexity as other cases are considered, is given in Appendix 1, where by equation (A3)

$$dPE/dR = p_0 \gamma_0(1 - q_0) \{ 2/R - (1 + \Delta R/R)/H_p \} (1 + \Delta R/R) \rho_{R+\Delta R}/\rho_0, \tag{11}$$

and where H_p is the density scale height at $R + \Delta R$.

In general $\Delta R/R \leq 0.1$, while $H_p \ll \frac{1}{2}R$, so that dPE/dR is negative. In a static medium, the circular tube floats steadily upwards. The terminal velocity is found by equating the aerodynamic drag and $-dPE/dR$:

$$\begin{aligned} C\rho_{R+\Delta R} v^2 a_* l_0(1 + \Delta R/R) \\ = C\rho_{R+\Delta R} v^2 a_0 [\rho_0 q_0 / \{ \rho_{R+\Delta R} q_*(1 + \Delta R/R) \}]^{\frac{1}{2}} l_0(1 + \Delta R/R) \\ = p_0 \pi a_0^2 l_0(1 - q_0) \{ (1 + \Delta R/R)/H_p - 2/R \} (1 + \Delta R/R) \rho_{R+\Delta R}/\rho_0 \end{aligned} \tag{12}$$

from (11), l_0 being the initial length of the tube axis. Thus we have

$$v = \zeta \{ a(1 - q_0) \}^{\frac{1}{2}}, \quad (13)$$

where

$$\zeta^2 = \frac{\pi P_0}{C \rho_0} \left(\frac{\rho_{R+\Delta R} q^*(1 + \Delta R/R)}{\rho_0 q_0} \right)^{\frac{1}{2}} \left(\frac{1 + \Delta R/R}{H_p} - \frac{2}{R} \right).$$

Effectively, we can write

$$\zeta^2 = \frac{\pi P_0}{C \rho_0} \left(\frac{\rho_{R+\Delta R}(1 + \Delta R/R)}{\rho_0} \right)^{\frac{1}{2}} \left(\frac{1 + \Delta R/R}{H_p} - \frac{2}{R} \right),$$

as q^*/q_0 is very close to unity.

Table 1. Terminal velocities for the floating of a circular tube in a static region

Magnetic flux is $Ba^2 = 1.5 \times 10^{17}$ Mx

Depth of $z_0 - \Delta R$ (Mm)	Values of $vC^{\frac{1}{2}}$ (cm s^{-1}) for				V_c (cm s^{-1})
	$B = 10^6$ G	10^5 G	3×10^4 G	10^4 G	
155	6.1×10^3	1.1×10^3	440	190	2.52×10^3
100	6.8×10^3	1.2×10^3	490	220	3.43×10^3

The value of ζ varies only slowly with height, from $303/C^{\frac{1}{2}} \text{ cm s}^{-1}$ at 62 Mm to $228/C^{\frac{1}{2}} \text{ cm s}^{-1}$ at 200 Mm, if we refer to a zero level at depth 155 Mm. Several values of v are given in Table 1 for flux fibres in which $Ba^2 = 1.5 \times 10^{17}$ Mx ($1 \text{ Mx} \equiv 10^{-8} \text{ Wb}$).

With $C \approx 1$, the terminal velocities for flux fibres with $B \lesssim 10^6$ G span the convective velocity. It will be shown in Section 6d that the extreme range of B is less than $10^4 - 1.5 \times 10^5$ G, so that the terminal velocities are all appreciably smaller than V_c . Thus, we might expect the motions of flux fibres to be dominated by convective motions.

The convective velocity drops rapidly to 41 cm s^{-1} near the base of the convective region. Here the convective motions are too weak to prevent floating. As a consequence, flux fibres concentric with the Sun are never carried down to such depths. If, as is commonly believed, the scale height of a convective cell is of the order of the pressure scale height, it has a typical vertical scale of ~ 80 Mm; the top lies around a depth of 100 Mm. Flux fibres forming the real spiral-shaped tubes are carried around by convective motions in the central part of the lower convection zone, where the gas is drifting slowly towards the equator.

When ropes form from the coalescence of up to 10^3 or even 10^4 fibres, as argued by Piddington (1975, 1976a), the terminal velocity for floating increases by a factor of up to ~ 10 , and usually exceeds V_c . In this case we might expect the motions of the ropes to be more-or-less independent of convective motions. These are rather premature expectations. It is necessary first to study the influence of perturbations, the simplest of which is in a horizontal plane.

(b) Horizontal Deformations and the Formation of Flux Ropes

Piddington (1975, 1976a) has stressed the significance of gently twisted flux ropes for explaining surface phenomena, without giving details as to how such ropes could

be formed. If a flux tube is deformed horizontally by convective motions of velocity v normal to its axis and on a scale L , the tube is distorted as in Fig. 2. A simple model is to replace the curve by an isosceles triangle of base $2L$ and height $2y$. The initial radius, length and volume a_0 , $l_0 (=2\pi R)$ and γ_0 become a_* , l_* and γ_* respectively after distortion, where

$$l_* = l_0 - 2L + 2L\{1 + (2y/L)^2\}^{\frac{1}{2}}. \tag{14}$$

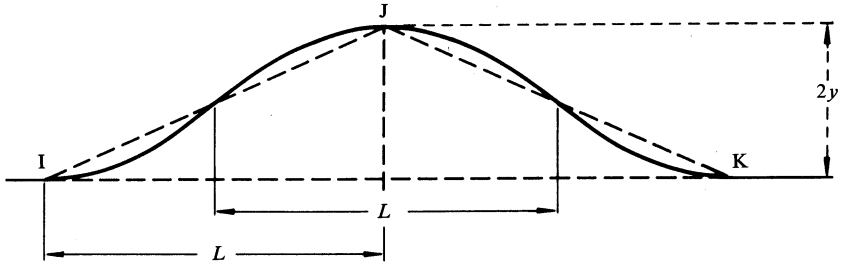


Fig. 2. Horizontal deformation of an otherwise circular flux tube concentric with the Sun. The solid curve represents the actual flux rope, the triangle IJK an approximation used in model calculations.

The conservation of mass during the short time interval involved implies that

$$l_0 a_0^2 q_0 = l_* a_*^2 q_* = l_* a_0^2 \{(1 - q_0)/(1 - q_*)\}^{\frac{1}{2}} q_*$$

from equation (2). Thus we get

$$1 - q_* = A_2 q_*^2,$$

where

$$A_2 = (1 - q_0)(l_*/l_0)^2/q_0^2. \tag{15}$$

From equation (10) the increase in PE due to the deformation is

$$\Delta PE = p_0 \gamma_0 (1 - q_0) \{(l_*/l_0)^2 q_*/q_0 - 1\}.$$

Since q_*/q_0 is very close to unity, it follows from (14) that

$$dPE/dy = p_0 \gamma_0 (1 - q_0) 16(l_*/l_0)y/l_0 L \{1 + (2y/L)^2\}^{\frac{1}{2}}. \tag{16}$$

The equilibrium distortion is found by equating the aerodynamic drag and dPE/dy :

$$C\rho_0 v^2 a_0 L = dPE/dy,$$

or

$$y/L \{1 + (2y/L)^2\}^{\frac{1}{2}} = C(\rho_0/p_0)(l_0/l_*)v^2 L/16\pi a_0(1 - q_0). \tag{17}$$

For large perturbations, (17) is not quite correct, since v should be the component of the drag velocity perpendicular to the axis of the deformed tube; it is however adequate for present purposes. A further approximation is now made by equating the drag velocity v to the convective velocity. Values of the deformation y when

an elementary fibre, taken to have $Ba_0^2 = 1.5 \times 10^{17}$ Mm, is at a depth 155 Mm, with v the convective velocity 2.52×10^3 cm s⁻¹ and $C = 1$, are given in Table 2 for disturbances on the two scales $L = 0.01 R_\odot$ and $0.1 R_\odot$. For weaker fields than those tabulated, the deformation exceeds the range of validity of (17).

Table 2. Horizontal deformation y produced in a flux fibre by a drag velocity equal to the convective velocity

Depth is 155 Mm and $C = 1$

B (G)	Values of y (cm) for	
	$L = 0.01 R_\odot$	$L = 0.1 R_\odot$
10^6	4.8×10^5	4.8×10^7
1.5×10^5	8.2×10^6	8.4×10^6
10^5	1.5×10^7	1.7×10^9
5×10^4	4.3×10^7	
3×10^4	9.5×10^7	
2×10^4	1.9×10^8	

We can now proceed to the mechanism of formation of flux ropes. If all flux fibres are identical and v is uniform everywhere, parallel fibres suffer uniform deformations and never meet. But with even minor variations in flux from fibre to fibre, the weaker tubes are deformed further. Slight up or down motions in the convection system can drag two fibres into contact. In most cases the deformations are likely to be on a large scale, especially with weaker rather than stronger fields as Table 2 indicates.

When tubes of force are dragged across one another at an appreciable angle, reconnection can occur by a process analogous to Petschek's (1964), as described in Part I. As long as the drag continues to pull the tubes into contact while reconnection proceeds, the speed of reconnection should be closely equal to that in Petschek's mechanism, about $0.01 V_A$ to $0.1 V_A$ where V_A is the Alfvén velocity. This type of interaction does not lead to rope formation, but if the angle between fibres is very small (e.g. ≤ 0.01 rad) reconnection is very slow, as Piddington (1976*b*) had pointed out. The component of magnetic tension available for withdrawing flux tubes from the reconnection zone then becomes very small. Thus, flux fibres which are twisted around one another at very small angles, in either sense of rotation, will reconnect only very gradually and partially, bonding the fibres where they are pulled together in a way quite probably resembling spot welding.

As the diameter of a rope increases, its ability to withstand deformation increases. Even so, there is the possibility of two ropes or incipient ropes winding around one another. Their individual fibres remain separate as in ropes made of hemp or wire, providing a substructure which may well be the basis for subsequent sunspot fragmentation associated with the development of light bridges.

The partial reconnection of gently twisted fibres in deep ropes inhibits the propagation of twists upwards along vertically deformed tubes such as Parker (1976) has claimed would destroy Piddington's twisted ropes.

(c) Vertical Deformations: Initiation of Floating of Flux Ropes

A model of the flux tube similar to that in Fig. 2 may be used to describe its deformation in a vertical plane, with two differences. The height of the isosceles triangle is now written as $2x$; and the initial length of flux tube l_0 is left unspecified

except that it be an arc of a circle concentric with the Sun. In the early stages of winding l_0 can be very long, but after the eruption of loops to form sunspots, it may be more appropriate to choose a much smaller value, for example $l_0 \approx R_\odot$.

The PE of the system is discussed in Appendix 2, where (see equation A5)

$$\frac{\partial \text{PE}}{\partial x} = \rho_0 \gamma_0 (1 - q_0) \frac{\partial}{\partial x} (G_1 F_1). \quad (18)$$

Now consider a perturbation of given height and arbitrary scale. It is readily shown that

$$(\partial/\partial x)(1/\sin \theta) = -\cos^2 \theta/x \sin \theta, \quad (19)$$

so that

$$\frac{\partial G_1}{\partial x} = \frac{2}{l \sin \theta} \left(2 \exp(-2xY) - \frac{\cos^2 \theta}{Yx} \{1 - \exp(-2xY)\} \right), \quad (20)$$

$$\frac{\partial F_1}{\partial x} = \frac{4}{l \sin \theta} \left(\exp(-x/H_p) - \frac{H_p}{x} \cos^2 \theta \{1 - \exp(-x/H_p)\} \right), \quad (21)$$

where $\sin \theta = 2x/(L^2 + 4x^2)^{1/2}$. Two special cases are of interest:

(a) When x is small we have

$$G_1 \frac{\partial F_1}{\partial x} + F_1 \frac{\partial G_1}{\partial x} = \frac{2L}{b_0} \left(-\frac{1}{2H_p} - Y + \text{terms in } x \right),$$

and thus $\partial \text{PE}/\partial x$ is negative for all scales of L .

(b) When the deep rope lies at a depth 155 Mm and $2x = 55$ Mm, calculation shows that $\partial \text{PE}/\partial x$ is positive for $L < 7.9 \times 10^9$ cm and negative for larger scales. For the latter, the perturbation continues to grow.

It can be shown that the development of a perturbation does not have a large effect on the deep tube as a whole. The results of Section 4a can be applied without further consideration.

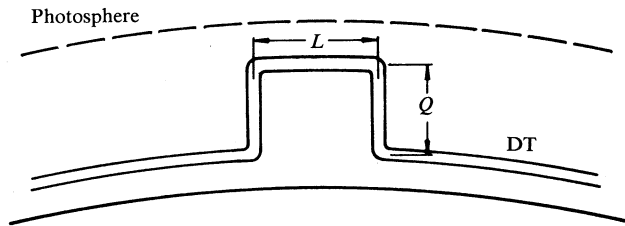


Fig. 3. Top-hat model used for studying the floating of flux loops in the upper half of the convection zone.

(d) Floating of Flux Tubes through Upper Convection Zone

At some stage the triangular model of the perturbation becomes inadequate. It is then better to use a top-hat model, in which an upper horizontal subtube of length L is connected to the deep tube by two vertical subtubes Q (see Fig. 3). As the

loop rises, gas spills into the subtubes Q which are extended in the process. If L is long enough, the gas spilled may exceed that required to fill the extensions, the surplus falling mainly into the deep tube DT. If L is too short, gas must be supplied, mainly from the deep tube. All traces of these physical phenomena are lost rapidly on calculating the changes in PE; but they are the essential aspects which decide whether or not floating will occur.

The potential energy is discussed in Appendix 3, where it is found from equation (A10) that the upward force on L is

$$\psi = -dPE/dz = -\rho_0 \pi a_0^2 (1 - q_0) [F_2 f_L (2 - L Y_{z_L}) / l_0 + G_2 \{ -(L/2 H_p) \exp(-z_L/2 H_p) + 2(p_L/\rho_0)^{1/2} \}]. \quad (22)$$

As $G_2 \approx 1$ and $F_2 \approx l_0$, equation (22) is roughly

$$\psi \approx -\rho_0 \pi a_0^2 (1 - q_0) \{ f_L (2 - L Y_{z_L}) + (p_L/\rho_0)^{1/2} (-L/2 H_p + 2) \}. \quad (23)$$

This is very different from the incorrect result obtained from the application of Archimedes' principle, namely $p_L \gamma_L (1 - q) / H_p$.

The relation (23) shows that L usually experiences an upthrust when L is long, but a downward force when L is short. The transition occurs in the approximate range $4H_p \lesssim L \lesssim 2/Y$. As examples, equation (22) shows that if the deep tube is at $z_0 = 155$ Mm, the transitions when L is at depth z are:

Depth of L	Transition length
$z = 10$ Mm	$L = 37$ Mm
100 Mm	250 Mm

The disagreement between the two models at depth 100 Mm is not too surprising, for this is where each might perform worst. Overall, we can see the general pattern in which very tiny perturbations occur on all scales, though only the larger can survive up to a depth of 100 Mm. At shallower depths the perturbations develop into well-defined loops, tapering in as they approach the surface. By a depth of 10 Mm they will continue to float upwards provided that $L > 37$ Mm. This size is a minimum, at which there is a neutral equilibrium, and L will exceed it in all cases where the loop floats.

The velocity of floating is found by equating the aerodynamic drag on a rope of N fibres and radius a_N :

$$C \rho v^2 a_N L = -dPE/dz.$$

With $L = 50$ Mm at a depth 10 Mm, then $\psi = -0.84 \rho_0 a_{N0}^2 (1 - q_0)$, where a_{N0} is the rope diameter at level z_0 . It is convenient to convert a_{N0} to a_N using equation (2), whence

$$C \rho v^2 a_N L = - \frac{0.84 p \pi a_N^2 (1 - q)}{\rho (p/\rho_0)^{1/2} L G_1} \quad \text{or} \quad v = 1.5 \times 10^3 \{ a_N (1 - q) / C \}^{1/2}.$$

With $1 - q = B^2/8\pi p$ and $a_N = 3.81 \times 10^{10} B^{-\frac{1}{2}}$ for a rope of 10^4 fibres each having $Ba^2 = 1.5 \times 10^{17} \text{ Mx}$, then $v = 7.1 \times 10^2 B^{\frac{3}{2}} C^{-\frac{1}{2}}$ or $7.1 \times 10^5 \text{ cm s}^{-1}$, if $B = 10^4 \text{ G}$ and $C = 1$. For this value of B , the rope diameter is 7.75 Mm , or about $\frac{3}{4}$ of the depth of the rope. Thus, the time for the rope to float through the surface is not very different from $2a_N/v$,

$$t = 1.1 \times 10^8 C/B^{\frac{5}{2}} = 1.1 \times 10^3 \text{ s} \quad \text{if again } C = 1.$$

There are observations of the time required for this process, which produces arch filament systems whose typical development requires a day or so, longer than our approximate calculation by a factor of ~ 100 . For the time scales to agree B would need to be $\sim 300 \text{ G}$, which is quite incompatible with the observed sunspot fields of $\sim 3000\text{--}4000 \text{ G}$. It is difficult to explain such a large difference unless the condition $T_i = T_e$ is inapplicable, so let us then examine case 2.

5. Floating of Flux Tubes: Case 2 with B Uniform with Height and $\rho_i = \rho_e$

(a) Introduction

In case 2, B is uniform with height, although this can be so only over a limited though possibly large range of height. Both Piddington (1976*b*) and Spruit and Ballegooijen (1982) have asserted that the equality of internal and external densities ensures neutral equilibrium, but this is not so. As in case 1, it is necessary to examine the changes in PE involved.

Because the mass of gas in the tube is fixed, any change in tube configuration causes a change in tube volume and in the uniform (but not invariable) field strength. The volume change is accompanied by a change in PE, assessed by

$$\Delta \text{PE} = \int p \, d\gamma. \quad (24)$$

The integral is to be taken over the whole tube. As before, it is necessary to calculate the tube radius a from the equation of mass invariance.

The two cases discussed in Sections 4*a* and 4*b* lead, with even less approximation than in case 1, to the same results as case 1; we do not need to give the analysis here.

(b) Vertical Deformation of a Flux Tube

Consider a flux tube or rope whose axis of length l_0 is concentric with the Sun. We suppose that it is perturbed upwards through a height $2x$, as in Section 4*c*. Appendix 4 discusses for the lower convection zone the potential energy derived from the triangular approximation and its variation with x (see equation A13). A little reduction yields

$$\partial G_2 / \partial x = 4(\sin \theta) / l_0,$$

$$\partial F_2 / \partial x = (2/l_0 \sin \theta) [2 \exp(-2x/H_p)$$

$$- (H_p \cos^2 \theta / x) \{1 - \exp(-2x/H_p)\}].$$

(a) When x is small, we have

$$G_2 \frac{\partial F_2}{\partial x} + F_2 \frac{\partial G_2}{\partial x} = - \frac{2L}{b_0 H_p} + \text{terms in } x,$$

and thus $\partial \text{PE} / \partial x$ is negative for all scales of L .

(b) When the deep rope lies at a depth 155 Mm and $2x = 55$ Mm, calculation shows that $\partial \text{PE} / \partial x$ is negative for $L \gtrsim 1.4 \times 10^{10}$ cm. Perturbations of scale larger than this will still float when they rise to a depth 100 Mm. Smaller scales cannot reach this level in the triangular model.

(c) *Floating of Flux Tubes through Upper Convection Zone*

A top-hat model is more appropriate in the upper convection zone, and the analysis is fairly simple. The mass in the deep tube is $\pi a^2 (b_0 - L) \rho_0$. In L the mass is $\pi a^2 L \rho_L$, and in the two tubes Q it is $2\pi a^2 \int_0^{z_L} \rho_j dj$. Then the equation of mass invariance is

$$\pi a_0^2 b_0 q_0 \rho_0 = \pi a^2 b_0 G_2, \tag{25}$$

where

$$G_2 = \rho_0(1 - L/b_0) + \rho_L L/b_0 + 2 \int_0^{z_L} \rho_j dj / b_0,$$

and thus

$$a^2 = a_0^2 q_0 \rho_0 / G_2.$$

In the deep tube, the contribution to ΔPE is $p_0 \pi a^2 (b_0 - L)$. In L it is $p_L \pi a^2 L$, and in the two tubes Q it is $2\pi a^2 \int_0^{z_L} p_j dj$. Thus, the total is

$$\begin{aligned} \Delta \text{PE} &= \pi a^2 \left(p_0 (b_0 - L) + p_L L + 2 \int_0^{z_L} p_j dj \right) - \text{const.} \\ &= \pi a^2 E - \text{const.}, \end{aligned}$$

where

$$E = p_0 (l_0 - L) + p_L L + 2 \int_0^{z_L} p_j dj.$$

From this we get

$$\partial \text{PE} / \partial z_L = (2\pi a \partial a / \partial z_L) E + \pi a^2 \partial E / \partial z_L.$$

Now we have

$$\begin{aligned} 2a da / dz_L &= -a_0^2 q_0 \rho_0 G_2^{-2} dG_2 / dz \\ &= -a^2 \rho_L (-L/H_p + 2) / b_0 G_2, \end{aligned}$$

where again H_p is the density scale height at the level of tube L , so that

$$2a da / dz_L = -\pi a^2 \frac{\rho_L}{b_0 G_2} E \left(-\frac{L}{H_p} + 2 \right) + \pi a^2 \left(-\frac{L}{H_p} + 2 \right) p_L;$$

that is,

$$\frac{1}{\pi a^2} \frac{d \text{PE}}{dz_L} = -\frac{\rho_L}{b_0 G_2} E \left(-\frac{L}{H_p} + 2 \right) + p_L \left(-\frac{L}{H_p} + 2 \right). \tag{26}$$

We let the deep tube lie at a depth 155 Mm and put $l_0 = R_{\odot}$, a value which can be regarded as allowing for the more-or-less vertical portions of the tube at either end. In the top-hat model, the scales on which floating occurs are:

Depth of L	Scales which float
100, 62, 24 Mm	All
15	$L < 15.6$ Mm
10	$L < 9.6$ Mm

As in case 1 there are differences from the triangular perturbation model when the perturbation has risen to a depth of 100 Mm. The latter was found able to float only on scales >140 Mm. This level is the one where the two models are at the limit of their applicability, and the differences should not be regarded as serious.

It is interesting that in case 2 the top-hat model predicts floating on all scales as the perturbation rises to a depth of 24 Mm, but above this only the smaller scales may float.

Case 2 is much more artificial than case 1 since it requires a very specific temperature difference below the external temperature, which varies as a function of height. Even so, a general pattern of floating can be described. Very small perturbations can develop on all scales, and certainly the larger of these, perhaps all, can grow up to depths of ~ 100 Mm. Above this they continue to grow on all scales until they reach depths of 24 Mm. Above this, the scales on which floating can occur become smaller, until by a depth of 10 Mm only scales of $\lesssim 9.6$ Mm survive. Thus in case 2 the perturbation tapers in towards the surface; the tube or rope would cut the surface with both sides lying within the diameter of a single sunspot. Clearly there are anomalies with case 2.

(d) Physical Principles in Establishing Temperature Gradient: Resolution of Arch Filament Lifetime

We consider the consequences of a top-hat tube of force floating upwards through the convection zone. For simplicity, we let $T_i = T_e$ at every level initially. If now the tube L rises, it expands because of the reduced external pressure, causing an overall increase in tube volume and adiabatic cooling. But there is in addition a pressure readjustment throughout the tube which involves an adiabatic temperature variation with height, similar to that in the external medium. The two effects are additive and the net result is a temperature in the flux tube everywhere lower than in its immediate surroundings.

The temperature commences to relax because of the inflow of radiation. The relaxation time may be assessed by making use of the results (and notation) given by Carslaw and Jaeger (1959) for the time variation of average temperature v inside an infinite cylinder of radius l whose surface is maintained at temperature V . Their Fig. 12, curve III, gives v/V in terms of the thermal diffusivity

$$\kappa = K/\rho C, \quad (27)$$

where K is the thermal conductivity and C the specific heat. The plotted curve applies specifically for a cylinder at zero initial temperature, but it is equally valid

for an initial uniform nonzero internal temperature. The time for the initial average temperature difference to relax by a factor of e^{-1} is given by $\kappa t/l^2 = 0.035$, or $t = 0.035l^2/\kappa$.

The ordinary thermal conductivity can be neglected by comparison with the radiative conductivity, for which Spruit (1977, p. 41) gave the expression

$$\kappa = 16\sigma T^3/3\kappa_R \rho, \quad (28)$$

where σ is the Stefan-Boltzmann constant and κ_R the Rosseland mean opacity per unit mass. For a fibril at depth 10 Mm and B as large as 10^5 G, then $l \equiv a = 1.225 \times 10^6$ cm, while with Spruit's (1974) values we have $\kappa = 1.04 \times 10^5$ (in c.g.s. units). Hence we get $t = 5.0 \times 10^6$ s \approx 60 days. For the average temperature to relax by 0.8 of the initial temperature difference requires 3.0×10^7 s, or about a year. For a rope of N fibres these times are increased by the factor N . Further, they are greater if $B < 10^5$ G or if the tube is deeper in the atmosphere. Therefore, we can disregard temperature changes due to the influx of radiation.

Surface observations can now tell us the domain in which the tube temperature lies. Floating cannot occur on the scale of arch filament systems if the temperature is as far below external as in the case 2, while the tube floats much too quickly if effectively at the external temperature. Clearly, the tube temperature is intermediate between cases 1 and 2. In this way the rate of floating is reduced and the observed lifetimes of arch filament systems can be satisfied readily. Theory is not yet developed sufficiently for the problem to be inverted, giving more exactly the temperature distribution from surface observations. Nevertheless, this emerges in Section 6.

6. Transport of Flux across the Sun's Surface

(a) Dispersal of Flux from Sunspots

Piddington (1975, 1976*a*, 1976*b*) has described how flux fibres unpeel from the ropes which form sunspots, and has produced diagrams showing the corresponding subsurface structures of ropes and fibres during and after sunspot decay. These concepts have strong observational backing.

It is well known that the surface magnetic elements reside mainly near the boundaries of supergranules, although they are also transported poleward over a time of 6–12 months during which most of the surface flux disappears. We now consider some of the problems of the interaction of the flux fibres with their surroundings.

A flux fibre which passes through the surface experiences a horizontal aerodynamic drag of order $C_p v^2 a H_\rho$ on that part of the fibre which projects upwards. Here ρ and H_ρ are the density and scale height at the level where the fibre is being drawn out, and v is the velocity of drag. If the rate at which the tube is being extended is e_v , then $0 < v < e_v$. During extension, gas must be supplied to fill the new volume. This can come either from deep within the convection zone, requiring the performance of work by the drag, or from the entry of gas into the tube, locally or from above during the long time available. Some of the processes involved have been studied by Giovanelli (1977). There are others, but all are insignificant by comparison with the rate of entry of gas by ohmic diffusion, which alone is of importance for the theory of the cycle. If the local supply is sufficient to fill the extending tube, the rate of extension is maximized, the only force to be overcome by the drag being the magnetic

tension $\frac{1}{8} B^2 a^2$. In this case we have

$$C\rho^2 a H_p \approx \frac{1}{8} B^2 a^2, \quad (29)$$

or

$$v \approx B(a/8C\rho H_p)^{\frac{1}{2}} \approx 11.7 B^{\frac{3}{4}} C^{-\frac{1}{2}} \text{ cm s}^{-1},$$

for a flux fibre in which $Ba^2 = 1.5 \times 10^{17} \text{ Mx}$ and for conditions appropriate to a depth of 10 Mm.

Observation indicates a typical time of 6 hours for the redistribution of the magnetic elements close to the boundaries of the new supergranules after the breakdown of the old. With typical distances of 7.5 Mm over which the elements must be transported, their velocities are $\sim 3.5 \times 10^4 \text{ cm s}^{-1}$. The typical supergranule velocities are $\sim 4 \times 10^4 \text{ cm s}^{-1}$. Thus the magnitude of v is $\lesssim 10^4 \text{ cm s}^{-1}$, and from equation (29), $B \lesssim 10^4 \text{ G}$ if $C = 1$.

There would be no possibility of the slow poleward motions transporting the magnetic elements but for the existence of the supergranule motions. It is still uncertain from observation whether the supergranules themselves drift slowly polewards, or whether there is rather, on average, a slight polewards redistribution of the elements after the breakdown of supergranules. The difference is immaterial for the present purposes. Both result on average in the polewards drift of the elements.

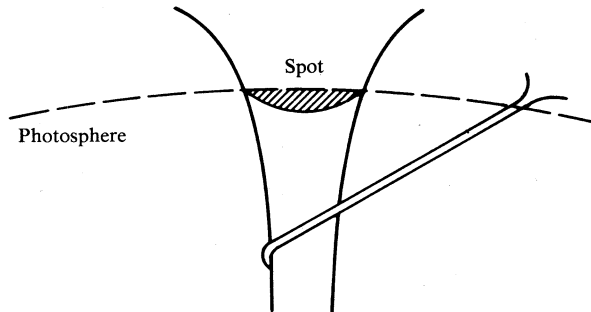


Fig. 4. Flux tube being drawn out from a sunspot.

The early stages of dispersal of flux tubes from sunspots involve a slightly different process. Here the flux tube is not dragged out horizontally, but is more as shown in Fig. 4. In this case the tube extension is quite small within say the first supergranule from the sunspot. Therefore the velocity of transport should be somewhat greater than normal in this region, but perhaps not sufficiently large to account for the observed enhancement across the moat. Another reason has been suggested by Piddington (1975, 1976a).

(b) Rate of Entry of Gas into Flux Tubes: Field Strength in Subsurface Fibrils during Poleward Transport

The volume of gas diffusing by ohmic dissipation into a unit length of a circular flux tube per second is given by $d(\pi a^2)/dt \approx 1/\sigma$, where σ is now the electrical conductivity (in emu). Under usual conditions this would result in the continuous

diffusion of flux into the surroundings. In the present case, a quite different situation occurs. The magnetic tube is being extended continuously, and gas flows along the tube to occupy the extensions. Instead of a continuous expansion of the tube, an equilibrium size is established whose properties we shall now explore.

If a tube of length l is being extended at velocity e_v by drag, a gas of volume ldt/σ enters in a time dt . During this time the tube extends to $l + e_v dt$ and the cross section changes to $\pi a^2 + d(\pi a^2)$. Then, we get

$$\pi a^2 l + l dt/\sigma = \{\pi a^2 + d(\pi a^2)\}(l + e_v dt),$$

or

$$d(\pi a^2)/dt = 1/\sigma - \pi a^2 e_v/l, \quad (30)$$

a relation that supposes zero gas is required from below.

A type of steady state is achieved when $d(\pi a^2)/dt = 0$; then

$$\pi a^2 = l/\sigma e_v. \quad (31)$$

With $Ba^2 = 1.5 \times 10^{17}$ Mx in a typical flux fibre, the field strength is

$$B = 1.5 \times 10^{17} \pi \sigma e_v/l \text{ G}. \quad (32)$$

The length of fibre is increased by contortions as in supergranules, so that $l = \alpha l_0$, where l_0 is the length in the absence of contortions. Then we get $e_v/l = 1/l_0$. Since $l_0 \sim R_\odot$, then $B \sim 1.0 \times 10^4$ G when we use Spruit's value of $\sigma = 7.6 \times 10^{-7}$ emu for a depth 10 Mm. This is in close agreement with the value Piddington (1975) inferred from observation, and implies that the extension of the flux tube involves little supply of gas from deeper regions. It is interesting that the rate of extension of the tube has dropped out of the expression for the field strength.

(c) Downward Transport of Flux Fibres in Polar Regions

When magnetic elements are carried to polar regions, the subsurface tubes joining them back to the ropes surviving from the dispersed sunspots remain subject to dragging around by convective motions or eddies. However, the small drift velocity superimposed on the larger convective motions is now downwards, and this is the overall direction in which the subsurface tubes are dragged. Their radii are far too small to allow floating to the surface in the presence of the strong convective motions.

How deep do they go? Close to the base of the convection zone the convective velocity becomes smaller than the velocity of floating (see Sections 4a and 5a), so that flux tubes can never reach such levels. On average they are carried around convective cells or eddies at a depth of ~ 155 Mm, about the centre level of the equator-ward flow.

The mass of gas diffusing into the tube per second is $\int (\rho/\sigma)\beta_D dz$, where β_D is a factor allowing for contortions in the tube. When the tube extends down to a depth of 155 Mm, the integral has the value $6.8 \times 10^{13} \beta_D \text{ gs}^{-1}$. It is interesting to compare this with the mass in the tube in cases 1 and 2. In case 1, a field 10^4 G at a depth 10 Mm implies 6.3×10^5 G at 150 Mm; the total mass turns out to be $9.7 \times 10^{20} \beta_D \text{ g}$. The characteristic time for filling the tube is 9×10^6 s, about 100

days. This is considerably shorter than the time required to carry the tube down. Suppose, for example, that the downflow occurs over a latitude belt of width $\frac{1}{5}R_{\odot}$, then the transport time is $\sim 10^8$ s or ~ 3 yr. In case 2, where the tube cross section is uniform, a field 10^4 G at a depth 10 Mm implies that $\pi a^2 = 4.7 \times 10^{13}$ cm² with a mass $4.7 \times 10^{13} \beta_D \int \rho dz = 3.0 \times 10^{22} \beta_D$ g down to 150 Mm. The characteristic time for filling the tube is 4.4×10^8 s, or 14 yr.

We saw earlier that the actual temperature distribution is intermediate between these two cases when a loop floats upwards. It is probably so in the polar downflow. The time to fill the tube is almost certainly intermediate between the above two extremes. The actual field strength follows from the next subsection.

(d) Field Strength in the Deep Tube

The bulk of the gas in a flux tube resides in the deep tube in the equatorward flow. Dragged out by differential rotation, the tube is spiral shaped. Ultimately it is wrapped around the Sun at a typical depth of 155 Mm. The ohmic diffusion of gas into this tube introduces several new problems.

As before, the equilibrium tube radius given by (31) is $a^2 = l/\pi\sigma e_v$, a relation which is deceptively simple. Flux ropes are being built up during winding, and at any one time N fibres will have been twisted together, initially rather loosely but later more tightly. At first sight, equation (31) suggests that the equilibrium diameter of a flux rope is independent of the number of its fibres, i.e. that the field strength increases greatly as the ropes grow.

It is by no means obvious that this will be so. For example, it is not clear that the equilibrium condition $d(\pi a^2)/dt = 0$ is reached in the case of thick ropes; (31) is then unlikely to be applicable.

There is also uncertainty as to the structure of the subsurface rope after several years of winding. It seems most likely that, at higher latitudes, winding of individual fibres is rather loose. At lower latitudes, the fibres become more tightly wound. On this basis, we can suppose that, down to about $\psi \approx 45^\circ$, the field strength is about the same as that of individual fibres. At lower latitudes, to about 30° , tubes of force receive gas which has entered the loosely wound fibres above $\psi \approx 45^\circ$, while relatively little gas diffuses directly into the much thicker rope at lower latitudes.

Within the range $\psi \gtrsim 45^\circ$, (31) gives $a^2 = l/\pi\sigma e_v$ where $l = 3.16 \times 10^7 n \bar{e}_v$, n being the number of years since polar latitudes were left, \bar{e}_v is the mean rate of extension of l in cm s⁻¹ and e_v the instantaneous rate of extension. Simple calculation shows that by $\psi = 45^\circ$ ($n = 4$), we have $\bar{e}_v = 0.73 e_v$, where

$$a^2 = 2.31 \times 10^7 n/\pi\sigma,$$

and where, for a depth 155 Mm, Spruit's conductivity is $\sigma = 1.165 \times 10^{-5}$ emu. Then, we get

$$a^2 = 2.52 \times 10^{12} \text{ cm}^2.$$

For a single fibre, with $Ba^2 = 1.5 \times 10^{17}$ Mx, we have

$$B = 6.0 \times 10^4 \text{ G}.$$

By continuity, this is also the field strength at the base of the downflow.

The field at latitudes down to the sunspot zone (30°) is found by noting that the total cross section, where $\phi < 45^\circ$, is πa_1^2 while, where $\phi \geq 45^\circ$, it is $N\pi a_2^2$. The two cross sections are effectively equal. If l_1 and l_2 are respectively the lengths of deep tubes from polar latitudes to $\phi < 45^\circ$ and to $\phi \approx 45^\circ$, the ratio of the corresponding volumes is simply l_1/l_2 , with a value of about 2 by 30° . Thus, B roughly doubles to 1.2×10^5 G by $\phi \approx 30^\circ$.

At lower latitudes, sections of flux rope are cut off increasingly as sunspot development proceeds. To estimate the field strength in these sections, we make the simple assumption that, on average, B is unchanged initially after the section is cut off. The length of tube available for gas entry is then reduced greatly, and as a consequence the field may not change much subsequently. Any significant inflow reduces B . Thus we have $B \leq 1.2 \times 10^5$ G.

7. Review and Discussion

In Part I and here we have considered the extent to which the main observed features of the sunspot and magnetic cycles can be explained in terms of surface and subsurface phenomena. A single coherent self-consistent scheme has emerged involving a new type of dynamo theory and covering:

- (i) the mechanism of reversal of the polar magnetic field;
- (ii) the method of transport of magnetic flux in the convection zone, including transport in regions of very slow drift velocities;
- (iii) the strength of fields in flux tubes throughout the convection zone;
- (iv) the mechanism whereby flux ropes are built up in the deeper convection zone, and the typical depth at which this takes place; and
- (v) conditions under which flux ropes will float to the surface to form sunspots.

The analysis has brought to light several physical phenomena which have been overlooked or handled incorrectly in previous studies, and render all previous analyses invalid. These include:

- (i) overemphasis on local properties of flux tubes rather than treating tubes as a whole;
- (ii) the failure of Archimedes' principle to describe the floating of flux tubes;
- (iii) the omission of the inflow of gas to flux tubes by ohmic dissipation as a crucial feature controlling their field strengths; and
- (iv) neglect of the dominant role of gas motions in transporting flux tubes when their velocities of floating are small compared with convective velocities.

Taken as a whole, these factors have been responsible for the very major differences between the results found here and those of earlier and contemporary workers in dynamo theory.

The main additional results are that:

- (i) the building of flux ropes occurs at depths of typically 150 Mm, field strengths being $\sim 10^4$ to 1.2×10^5 G;
- (ii) perturbations which will float to the surface can develop only when hundreds or thousands of flux fibres have been twisted to one another at angles of order 0.01 rad or less to form flux ropes;

- (iii) the field drops off with height in a flux tube, but not as rapidly as when internal and external temperatures are identical at all levels;
- (iv) just as differential rotation distorts flux tubes into a spiral shape, so these flux tubes react to reduce differential rotation. A good representation is found for the phase pattern in the torsional oscillation and its relation to the sunspot cycle. The amplitude is complicated but satisfying agreement with observation emerges from the discussion for latitudes above the sunspot zone. At lower latitudes the phenomenon becomes more complicated and is not treated here;
- (v) the Hale and Spörer laws follow readily.

The whole analysis has been made on the basis of perturbations having the form of simple models. There remains the need to undertake more exact analyses so as to provide greater insight into these various phenomena.

References

- Carlsaw, H. S., and Jaeger, J. C (1959). 'Conduction of Heat in Solids', p. 102 (Clarendon: Oxford).
- Giovanelli, R. G. (1977). *Sol. Phys.* **52**, 315.
- Giovanelli, R. G. (1982). *Sol. Phys.* **80**, 21.
- Giovanelli, R. G. (1985). *Aust. J. Phys.* **38**, 1045.
- Parker, E. N. (1955). *Astrophys. J.* **121**, 491.
- Parker, E. N. (1976). *Astrophys. Space Sci.* **44**, 107.
- Parker, E. N. (1979). *Astrophys. J.* **231**, 250; **232**, 282.
- Petschek, H. E. (1964). Symp. on the Physics of Solar Flares (Ed. W. N. Haas), p. 425 (NASA: Washington, D.C.).
- Piddington, J. H. (1975). *Astrophys. Space Sci.* **40**, 73.
- Piddington, J. H. (1976a). In 'Basic Mechanisms of Solar Activity', IAU Symp. No. 71 (Eds V. Bumba and J. Kleczek), p. 389 (Reidel: Dordrecht).
- Piddington, J. H. (1976b). *Astrophys. Space Sci.* **45**, 47.
- Spruit, H. C. (1974). *Sol. Phys.* **34**, 277.
- Spruit, H. C. (1977). Magnetic flux tubes and transport of heat in the convection zone of the Sun. Ph.D. Thesis, University of Utrecht, p. 41.
- Spruit, H. C. (1981). *Astron. Astrophys.* **98**, 155; **102**, 129.
- Spruit, H. C., and Ballegooijen, A. A. (1982). *Astron. Astrophys.* **106**, 58.

Appendix 1. Mass Invariance and Potential Energy Changes in a Circular Tube of Force always Concentric with the Sun

Let a toroidal tube of force of circular cross section, with radius a_0 , lie at distance R from the Sun's centre. Suppose now it rises by ΔR , with the original volume, pressure ratio, external density and tube radius changing from $\gamma_0, q_0, \rho_0, a_0$ to $\gamma_*, q_*, \rho_*, a_*$. Then the conservation of mass during the short interval involved implies

$$\gamma_* q_* \rho_* = \gamma_0 q_0 \rho_0,$$

that is,

$$\pi a_0^2 2\pi R(1 + \Delta R/R) q_* \rho_0 (\rho_{\Delta R}/\rho_0) = \pi a_0^2 2\pi R q_0 \rho_0.$$

Thus, we get

$$a_0^2 \{(1 - q_0)/(1 - q_*)\}^{\frac{1}{2}} (p_0/p_{R+\Delta R})^{\frac{1}{2}} (1 + \Delta R/R) q_* (\rho_{R+\Delta R}/\rho_0) = a_0^2 q_0$$

from equation (2), so that

$$1 - q_* = A_1 q_*^2, \quad (A1)$$

where

$$A_1 = (1 - q_0)(1 + \Delta R/R)^2 (\rho_{R+\Delta R}/\rho_0)^2 (p_0/p_{R+\Delta R})/q_0^2$$

$$= (1 - q_0)(1 + \Delta R/R)^2 \exp(-2Y \Delta R)/q_0^2,$$

and where $Y = 1/H_p - 1/2H_p$.

The increase in potential energy PE may now be written as

$$\Delta PE = p_{R+\Delta R} \pi a_*^2 2\pi R(1 + \Delta R/R)(1 - q_*) - p_0 \gamma_0(1 - q_0)$$

$$= p_0 \gamma_0(1 - q_0)[(1 + \Delta R/R)^3 \{(1 - q_0)/(1 - q_*)\}^{1/2} (\rho_{R+\Delta R}/\rho_0)^2 (p_0/p_{R+\Delta R})^{1/2}$$

$$\times (q_*/q_0)^2 - 1]$$

from equation (2), which reduces to

$$\Delta PE = p_0 \gamma_0(1 - q_0)\{(1 + \Delta R/R)^2 (\rho_{R+\Delta R}/\rho_0) q_*/q_0 - 1\} \tag{A2}$$

from (A1). Then we get

$$dPE/dR = p_0 \gamma_0(1 - q_0)\{2/R - (1 + \Delta R/R)/H_p\}(1 + \Delta R/R)\rho_{R+\Delta R}/\rho_0, \tag{A3}$$

since q_*/q_0 is effectively unity. Note again that H_p is the density scale height at $R + \Delta R$.

Appendix 2. Mass Invariance and Potential Energy Changes in a Vertical Triangular Deformation: Case 1 with $T_i = T_e$

Consider a deformation similar to that shown in Fig. 2, except that the isosceles triangle now lies in a vertical plane and its height is $2x$. The initial length of arc l_0 is now arbitrary, and the base length of the deformation is $2L$. After the perturbation develops, the unperturbed part has a mass $\pi a_*^2(l_0 - 2L)\rho_0 q_*$, where a_* is the tube radius at zero height and q_* the pressure ratio. In an element of length $ds = dz/\sin \theta$, where θ is the base angle of the triangle, the mass in the perturbation is $\pi a_z^2(dz/\sin \theta)\rho_z q_*$. Integrated over both sides of the perturbation, its mass is $2\pi a_*^2 \rho_0 q_* \{1 - \exp(-2xY)\}/Y \sin \theta$. Thus, the mass invariance equation becomes

$$\pi a_0^2 l_0 \rho_0 q_0 = \pi a_*^2(1 - 2L)\rho_0 q_* + 2\pi a_*^2 \rho_0 q_* \{1 - \exp(-2xY)\}/Y \sin \theta$$

$$= \pi a_0^2 \rho_0 q_* \{(1 - q_0)/(1 - q_*)\}^{1/2} [l_0 - 2L + 2\{1 - \exp(-2xY)\}/Y \sin \theta]$$

from equation (2). Then we have

$$1 - q_* = A_3 q_*^2,$$

where

$$A_3 = [1 - 2L/l_0 + 2\{1 - \exp(-2xY)\}/l_0 Y \sin \theta]^2 (q_*/q_0)^2 (1 - q_0).$$

Again we replace $(q_*/q_0)^2$ by unity, obtaining

$$1 - q_* = G_1^2(1 - q_0), \tag{A4}$$

where

$$G_1 = 1 - 2L/l_0 + 2\{1 - \exp(-2xY)\}/l_0 Y \sin \theta.$$

After development of the perturbation, the PE consists of two parts. The part due to the residue of the circular arc is $p_0 \pi a_*^2 (l_0 - 2L)(1 - q_*)$. To derive the contribution due to the perturbation, we note that the mass $dM_*(1 - q_*)$ is effectively expelled from $ds = dz/\sin \theta$, where

$$dM_* = \pi a_*^2 \rho_z dz/\sin \theta = \pi a_*^2 \exp(-z/Y) dz/\sin \theta.$$

Then the PE of the perturbation alone is

$$\begin{aligned} 2\pi \int_0^{2x} p_z a_*^2 (1 - q_*) dz/\sin \theta &= 2\pi p_0 a_*^2 (1 - q_*) \int_0^{2x} \exp(-z/2H_p) dz/\sin \theta \\ &= 2\pi p_0 a_*^2 (1 - q_*) \{1 - \exp(-x/H_p)\} 2H_p/\sin \theta. \end{aligned}$$

The total increase in PE can be expressed as

$$\begin{aligned} \Delta PE &= p_0 \pi a_0^2 \{(1 - q_0)/(1 - q_*)\}^{\frac{1}{2}} l_0 (1 - q_*) \\ &\quad \times [1 - 2L/l_0 + 4H_p \{1 - \exp(-x/H_p)\}/l_0 \sin \theta] - p_0 a_0^2 l_0 (1 - q_0) \\ &= p_0 \gamma_0 (1 - q_0) (G_1 F_1 - 1) \end{aligned} \tag{A5}$$

from (A4), where

$$F_1 = 1 - 2L/l_0 + 4H_p \{1 - \exp(-x/H_p)\}/l_0 \sin \theta.$$

Appendix 3. Mass Invariance and Potential Energy Changes in a Top-hat Model Perturbation: Case 1 with $T_i = T_e$

A large perturbation may be studied using a top-hat model with an upper horizontal subtube of length L connected to the deep tube DT by two vertical subtubes Q (see Fig. 3). For simplicity, DT is taken to be straight rather than curved.

The mass in the initial deep tube was $\pi a_0^2 l_0 q_0 \rho_0$. After loop formation, the mass becomes $\pi a_{DT}^2 (l_0 - L) q \rho_0$, where a_{DT} is its new radius and q the new value of p_i/p_e . The mass of L is $\pi a_L^2 L q \rho_L$ where ρ_L is the external density at the level of tube L . The mass of the two tubes Q is $2\pi \int_0^{z_L} a_j^2 q \rho_j dj$. Then, we get

$$\begin{aligned} \pi a_0^2 l_0 q_0 \rho_0 &= \pi a_{DT}^2 (l_0 - L) q \rho_0 + \pi a_L^2 L q \rho_L + 2\pi \int_0^{z_L} a_j^2 q \rho_j dj \\ &= \pi a_0^2 q \{(1 - q_0)/(1 - q)\}^{\frac{1}{2}} \left\{ (l_0 - L) \rho_0 + (p_0/p_L)^{\frac{1}{2}} L \rho_L + 2 \int_0^{z_L} \rho_j (p_0/p_j)^{\frac{1}{2}} dj \right\} \end{aligned}$$

from equation (2). Thus, we find

$$\{(1 - q)/(1 - q_0)\}^{\frac{1}{2}} q_0/q = G_2, \tag{A6}$$

where $G_2 = \{(l_0 - L) + Lf_L + 2f_Q\}/l_0$, and where

$$f_L = f_z(z = z_L), \quad f_z = (\rho_z/\rho_0)(p_0/p_z)^{\frac{1}{2}} = \exp\left(-\int_0^z Y_j dj\right), \quad f_Q = \int_0^{z_L} f_z dz.$$

The factor q_0/q in (A6) is very close to unity and may be omitted safely, so that

$$1 - q = G_2^2(1 - q_0). \quad (\text{A7})$$

The variation of q during floating is thus

$$\begin{aligned} dq/dz &= -(1 - q_0) 2 G_2 dG_2/dz \\ &= -(1 - q_0) 2 G_2 f_L(2 - LY)/l_0. \end{aligned} \quad (\text{A8})$$

The three terms within the braces in G_2 give respectively the relative masses in the deep tube, the horizontal subtube L , and the two vertical tubes Q . In general the major part lies in DT, with the least in L , while $G_2 \approx 1$.

Before loop development, the PE of the system is

$$p_0 \gamma_0(1 - q_0) = p_0 \pi a_0^2 l_0(1 - q_0).$$

After loop development, equations (2) and (A6) convert the PE of DT to

$$p_0 \pi a_{DT}^2(l_0 - L)(1 - q) = p_0 \pi a_0^2(1 - L)(1 - q_0) G_2.$$

The PE of tube L is

$$p_L \pi a_L^2 L(1 - q) = p_0 \pi a_0^2 L(1 - q_0)(p_L/p_0)^{\frac{1}{2}} G_2,$$

while that of the tubes Q is

$$2 \int_0^{z_L} p_z \pi a_z^2(1 - q) dz = 2 p_0 \pi a_0^2(1 - q_0) G_2 \int_0^{z_L} (p_z/p_0)^{\frac{1}{2}} dz.$$

Thus, we have

$$\text{PE} = p_0 \pi a_0^2(1 - q_0) G_2 F_2, \quad (\text{A9})$$

where

$$F_2 = l_0 - L + L(p_L/p_0)^{\frac{1}{2}} + 2 \int_0^{z_L} (p_z/p_0)^{\frac{1}{2}} dz.$$

Then, the upward force on L is

$$\begin{aligned} \psi &= -d\text{PE}/dz = -p_0 \pi a_0^2(1 - q_0)[F_2 f_L(2 - LY_{z_L})/l_0 \\ &\quad + G_2\{- (L/2H_p) \exp(-z_L/2H_p) + 2(p_L/p_0)^{\frac{1}{2}}\}]. \end{aligned} \quad (\text{A10})$$

Appendix 4. Mass Invariance and Potential Energy Changes in a Vertical Triangular Deformation: Case 2 with $\rho_i = \rho_e$

With the same geometry as in Section 4c, the mass in the initial tube of length l_0 with tube radius a_0 is $\pi a_0^2 l_0 q_0 \rho_0 = \gamma q_0 \rho_0$. Here the ratio q_0 is used on the assumption that the tube is initially isothermal with its surroundings.

After perturbation, case 2 requires the tube radius to be uniform everywhere. The mass in the unperturbed portion of the tube is $\pi a^2(l_0 - 2L)\rho_0$. In the model

perturbation, the mass in an element of length $ds = dz/\sin \theta$ is $\pi a^2 \rho_z dz/\sin \theta$, where θ is the base angle of the triangle. Thus, the mass in the two inclined sides is

$$(2\pi a^2/\sin \theta) \int_0^{2x} \rho_0 \exp(-z/H_p) dz \quad \text{or} \quad 2\pi a^2 \rho_0 H_p \{1 - \exp(-2x/H_p)\}/\sin \theta,$$

if the scale height is taken as uniform over the height of the perturbation. Then, the mass equation becomes

$$\begin{aligned} \pi a_0^2 l_0 q_0 \rho_0 &= \pi a^2 (l_0 - 2L) \rho_0 + 2\pi a^2 \rho_0 H_p \{1 - \exp(-2x/H_p)\}/\sin \theta \\ &= \pi a_0^2 \{(1 - q_0)/(1 - q)\}^{\frac{1}{2}} [l_0 - 2L + 2H_p \{1 - \exp(-2x/H_p)\}/\sin \theta], \end{aligned}$$

where q is the ratio of internal and external pressures at the level of the deep tube. Thus, we have

$$1 - q = \frac{1 - q_0}{q_0^2} \left(1 - \frac{2L}{l_0} + \frac{2H_p}{l_0 \sin \theta} \{1 - \exp(-2x/H_p)\} \right)^2. \quad (\text{A11})$$

The PE of the unperturbed section of the tube is $\Delta PE_w = p_0 \pi a^2 (1 - 2L)(1 - q)$. In the perturbation, dz contributes an amount $dPE_p = 2p_z \pi a^2 (dz/\sin \theta)(1 - q_z)$. Integrated over the perturbation, the PE contribution is $(2\pi a^2) \int_0^{2x} p_z (1 - q_z) dz$. However, we have

$$a^2 = a_z^2 = a^2 \left(\frac{1 - q}{1 - q_z} \frac{p}{p_z} \right)^{\frac{1}{2}},$$

so that $p_z (1 - q_z) = p(1 - q) = p_0 (1 - q_0)$, and thus the contribution is

$$\begin{aligned} \Delta PE_p &= (2\pi a_0^2 p_0/\sin \theta) \int_0^{2x} (1 - q) dz = 2\pi a_0^2 p_0 (1 - q_0) \{(1 - q)/(1 - q_0)\}^{\frac{1}{2}} 2x/\sin \theta \\ &= 2\pi a_0^2 p_0 (1 - q_0) \left(1 - \frac{2L}{l_0} + \frac{2H_p}{l_0 \sin \theta} \{1 - \exp(-2x/H_p)\} \right) 2x/q_0 \sin \theta. \end{aligned}$$

Then we get

$$\Delta PE = \Delta PE_w + \Delta PE_p = (p_0/q_0) \pi a_0^2 (1 - q_0) l_0 (G_2 F_2 - \text{const.}), \quad (\text{A12})$$

where

$$F_2 = 1 - 2L/l_0 + 2H_p \{1 - \exp(-2x/H_p)\}/l_0 \sin \theta,$$

$$G_2 = 1 - 2L/l_0 + 4x/l_0 \sin \theta,$$

and thus

$$\partial PE/\partial x = (p_0/q_0) \gamma_0 (1 - q_0) \partial(G_2 F_2)/\partial x. \quad (\text{A13})$$

